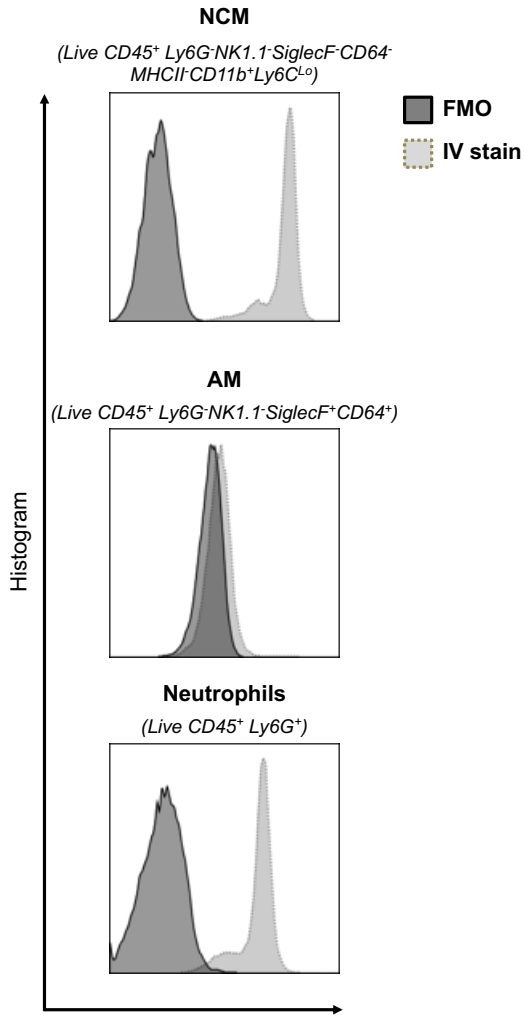

Figure S1. Staining protocol to identify intravascular vs. extravascular cells in lungs by flow cytometry. Resting mice were injected with 1.2 µg of (APC) labeled anti-CD45 (30-F11) by retro-orbital injection 3 minutes prior to euthanasia. The lung digests were then stained with (FITC)-labeled anti-CD45 (30-F11). Nonclassical monocytes (NCM) which are found in the intravascular compartment stained positively for (APC)-CD45 (IV), while alveolar macrophages (AM) which are found exclusively in the alveolar space stained negatively. Neutrophils, in a resting lung, can be found mostly in the intravascular compartment (98%).

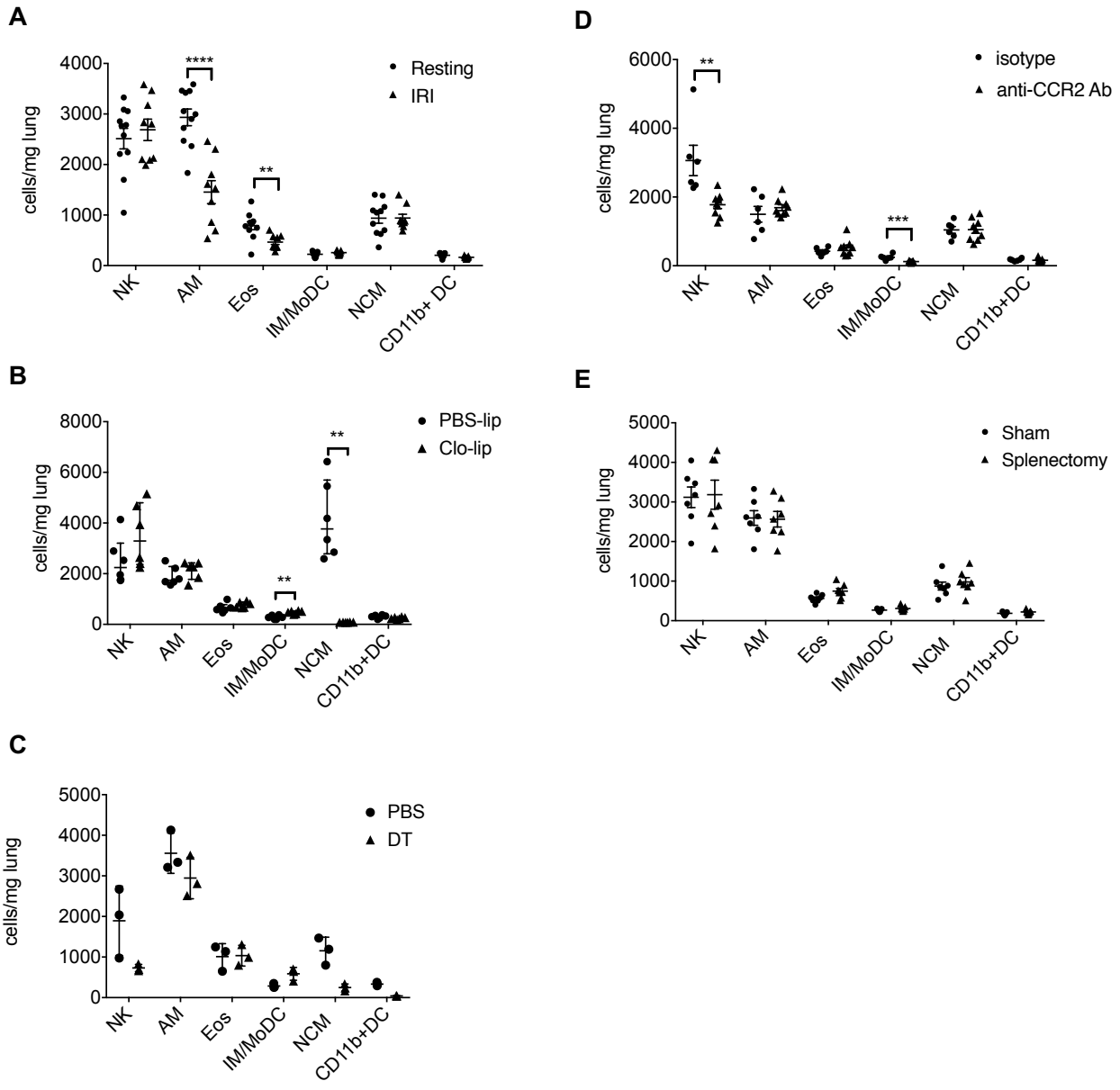

Figure S2. Changes in lung myeloid cell populations after hilar clamp-mediated IRI across treatment groups. Changes in myeloid cell populations in **(A)** IRI vs. resting mice, **(B)** Clo-lip vs. PBS-lip, **(C)** DT (CD11b-DTR mouse) vs. PBS, **(D)** anti-CCR2 Ab vs. isotype control and **(E)** splenectomy vs. sham splenectomy in resting mice. Data are expressed as median with interquartile range. *n*=3-11 per group. **P<0.01 and ****P<0.0001 by Mann-Whitney U test. NK: NK cells; AM: alveolar macrophages; Eos:

eosinophils; IM: interstitial macrophages; MoDC: monocyte-derived dendritic cells; NCM: non-classical monocytes; DC: dendritic cells

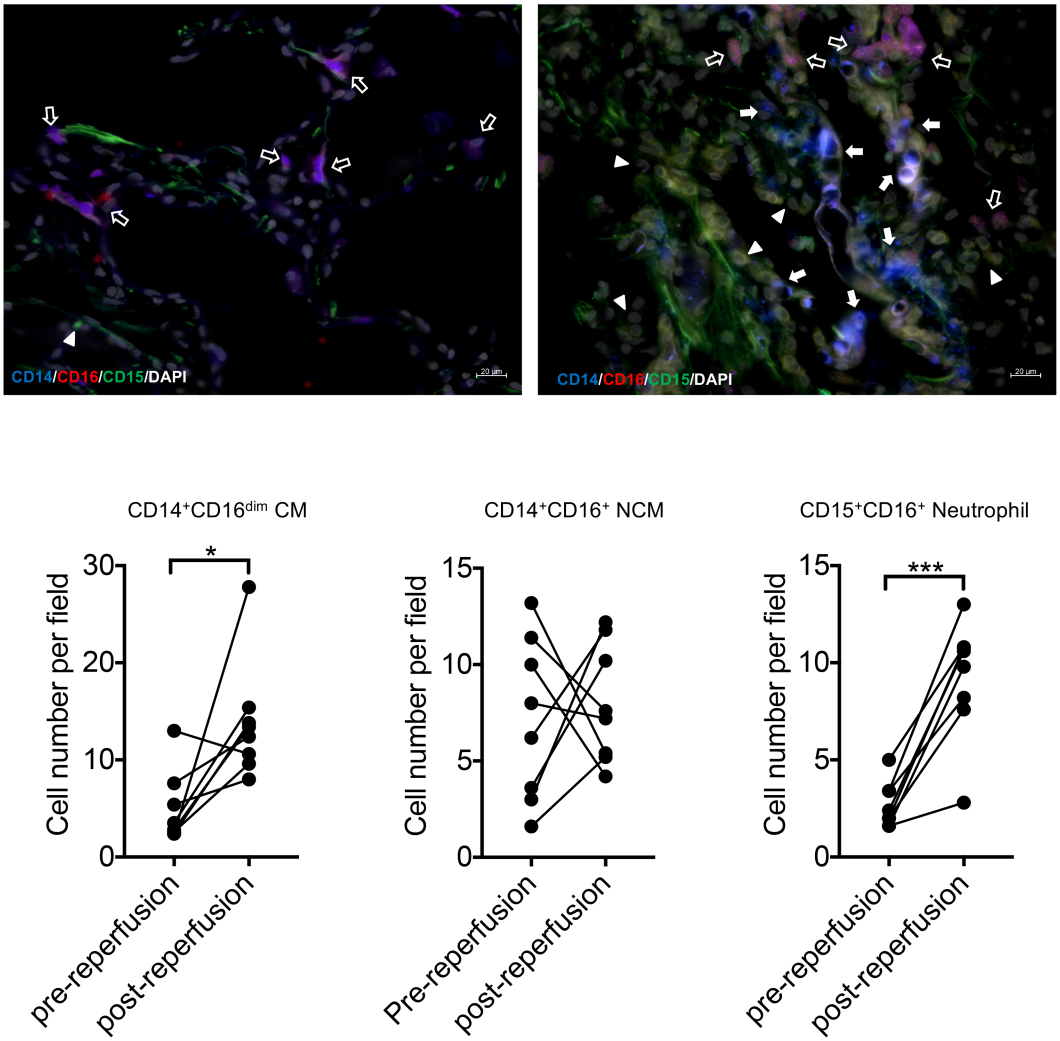

Figure S3. Changes in monocyte populations and neutrophils in human lung grafts pre- and post-reperfusion. Frozen tissues of human donor lung grafts were stained with antibodies specific for CD14 (blue), CD15 (green) and CD16 (red) at the conclusion of cold ischemic storage and 2 hours after reperfusion. Nuclei were counterstained with DAPI (white). Classical monocytes ($CD14^{+}CD16^{dim}$) (solid arrows), nonclassical monocytes ($CD14^{+}CD16^{+}$) (open arrows) and neutrophils ($CD15^{+}CD16^{+}$) (solid arrowheads) were counted per high power fields and quantified in samples from 8 patients

pre- and post-reperfusion. Scale bar = 20 μm. Images were taken with a 40x water immersion objective lens. *p<0.05 and ***p<0.001 by paired t-test.

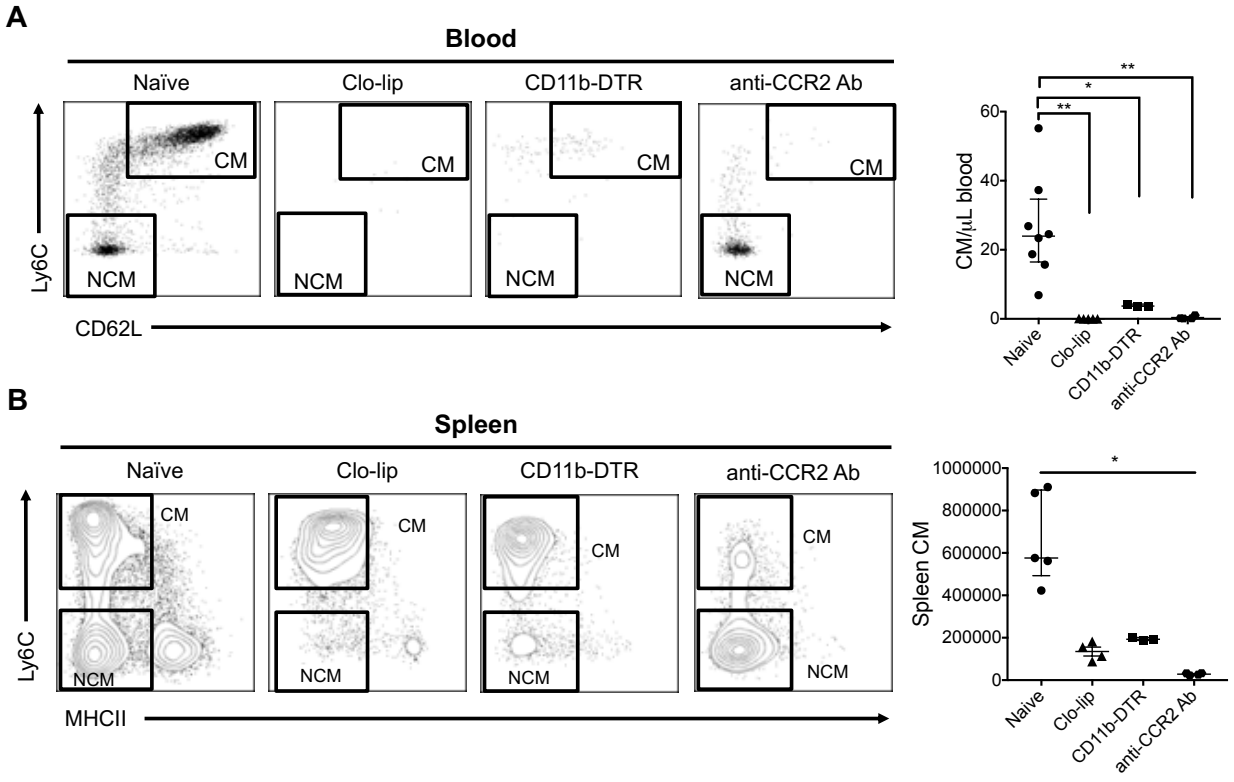

Figure S4. The effect of monocyte depletion strategies on circulating CM in resting mice. (A) Blood: Representative flow plots and classical monocyte levels in blood 24 hours after treatment with intravenous Clo-lip, intraperitoneal DT (CD11b-DTR), or intravenous anti-CCR2 antibody. *n*=3-8 mice per group. Data expressed as median with interquartile range, *P<0.05, **P<0.01 by Mann-Whitney U test **(B)** Spleen: Representative flow plots and classical monocyte levels in spleen 24 hours after treatment with intravenous Clo-lip, intraperitoneal DT (CD11b-DTR), or intravenous anti-CCR2 antibody. *n*=5 mice per group. Data are expressed as median with interquartile range. *p<0.05 by Mann-Whitney U test.

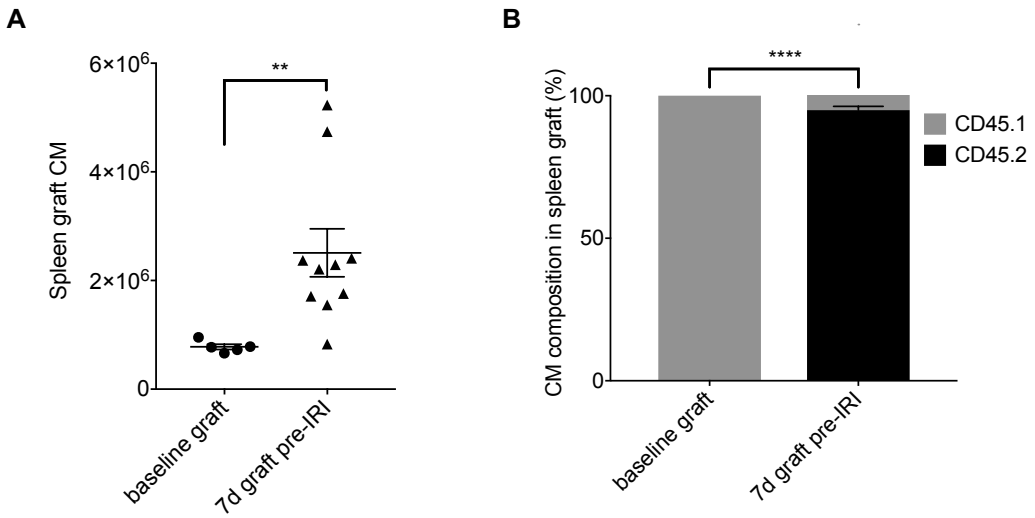

Figure S5. Spleen graft composition 7 days after heterotopic spleen transplant. Congenic heterotopic spleen transplant (CD45.1 donor into CD45.2 recipient) was performed as described in the methods. **(A)** Quantification of resting spleen graft classical monocytes before implantation (baseline) and 7 days post-transplant. Data are expressed as median with interquartile range. *n*=5-10 mice per group. **p<0.01 by Mann-Whitney U test. **(B)** Composition of donor-derived (CD45.1) vs recipient-derived (CD45.2) classical monocytes in graft at baseline and 7 days after transplant. Data expressed as mean ± SEM. ****P<0.0001, *n*=5-10 mice per group. Unpaired t-tests were used for pairwise comparisons of the means.

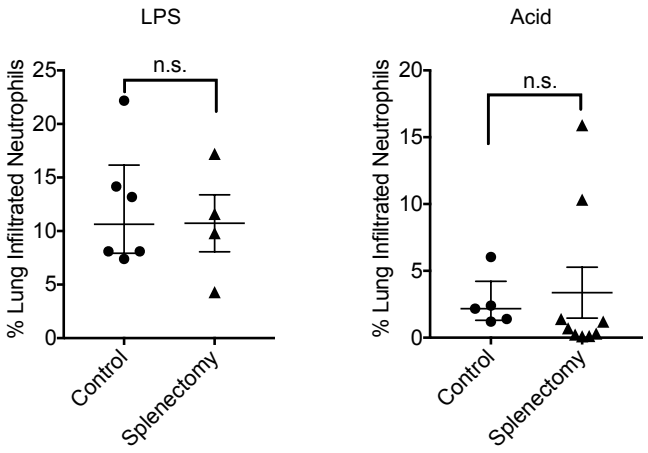

Figure S6. Effect of splenectomy on neutrophil extravasation in lipopolysaccharide (LPS) and acid-induced lung injury. (A) LPS (2 μg/g) or **(B)** 0.1 N hydrochloric acid (50 μL) were delivered intratracheally into asplenic vs. spleen-intact mice and neutrophil extravasation determined as previously described. *n*=4-9 mice per group. Data expressed as median with interquartile range and analyzed with Mann-Whitney U test (n.s.: not significant).

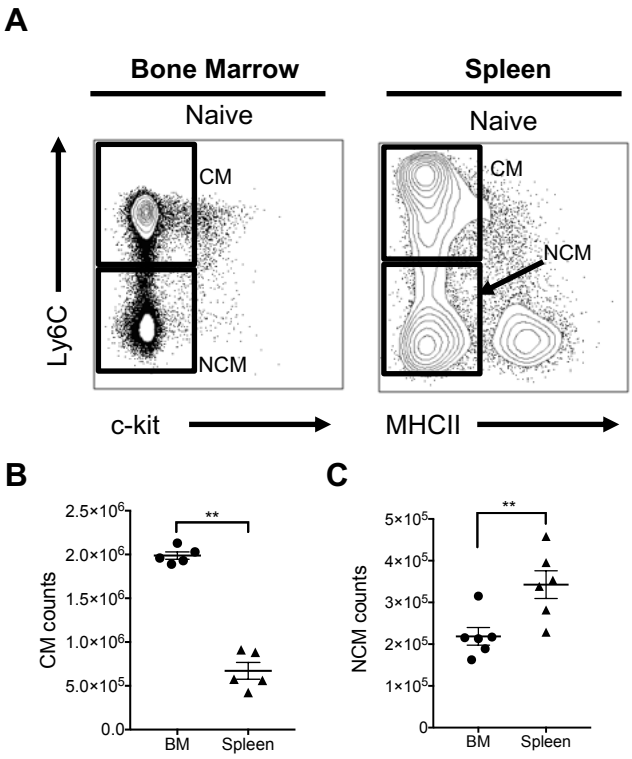

Figure S7. Classical and nonclassical monocytes in bone marrow and spleen at baseline. (A) Representative flow cytometry plots of classical and nonclassical monocytes in bone marrow (*left)* and spleen (*right)* at resting state. Bone marrow monocytes were gated on live $CD11b^{+}Ly6G^{-}NK1.1^{-}$ cells. Splenic monocytes were gated on live $F4/80^{-}CD4^{-}CD8^{-}CD19^{-}Ly6G^{-}NK1.1^{-}CD11c^{-}MHCII^{-}SSC^{low}CD11b^{+}$ cells. Spleen samples were diluted 1:15 while the bone marrow samples were diluted 1:5. Quantification of **(B)** classical monocytes (CM) and **(C)** nonclassical monocytes (NCM) in bone marrow (2 femurs and 2 tibiae) and spleen during resting state. Data are expressed as median with interquartile range. *n*=5-6 mice per group. **p<0.01 by Mann-Whitney U test.

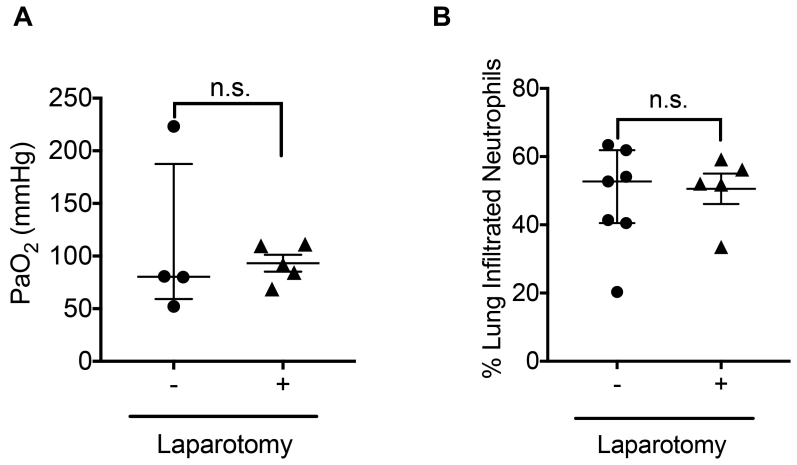

Figure S8. Comparison of wildtype lung recipients to recipients that underwent sham laparotomy. (A) Arterial blood oxygenation was assessed and **(B)** percentage of extravasated neutrophils were determined in lung grafts 24 hours after transplantation of B6 CD45.1^{+} lungs into control congenic B6 CD45.2^{+} recipients or B6 CD45.2^{+} hosts that underwent a sham laparotomy. Data expressed as median with interquartile range and analyzed with Mann-Whitney U test (n.s.: not significant)(*n*=4-7 per group).

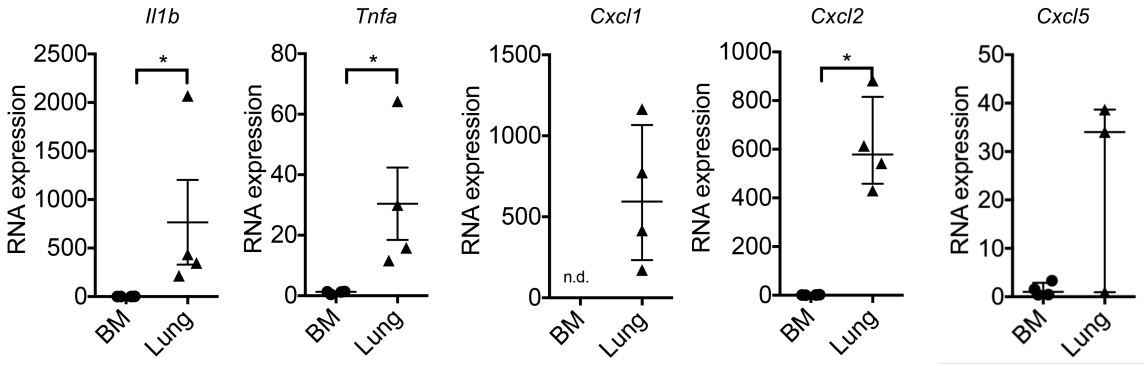

Figure S9. Expression levels of pro-inflammatory cytokine and chemokines in bone marrow and lung monocytes at baseline. Classical monocytes were isolated from the bone marrow or lung of resting B6 CD45.2^{+} mice and analyzed for the expression of *Il1b*, *Tnfa*, *Cxcl1*, *Cxcl2* and *Cxcl5* transcripts by quantitative real-time PCR. Data are expressed as median with interquartile range, n=4 for each compartment with one statistical outlier for *Cxcl5* in the lung excluded from the analysis; *p<0.05 by Mann-Whitney U test, n.d. = not detectable.

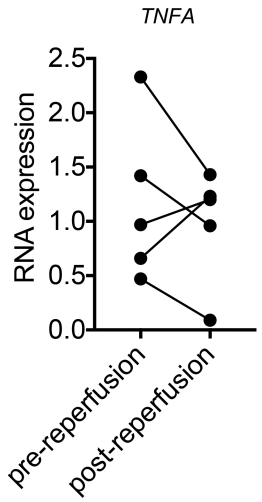

Figure S10. Levels of TNF-α in human donor lung grafts pre- and post-reperfusion.

Expression levels of TNF-α in human donor grafts pre- and post-reperfusion were assessed by quantitative PCR. For each group, n= 5. Data not significant by paired t-test.

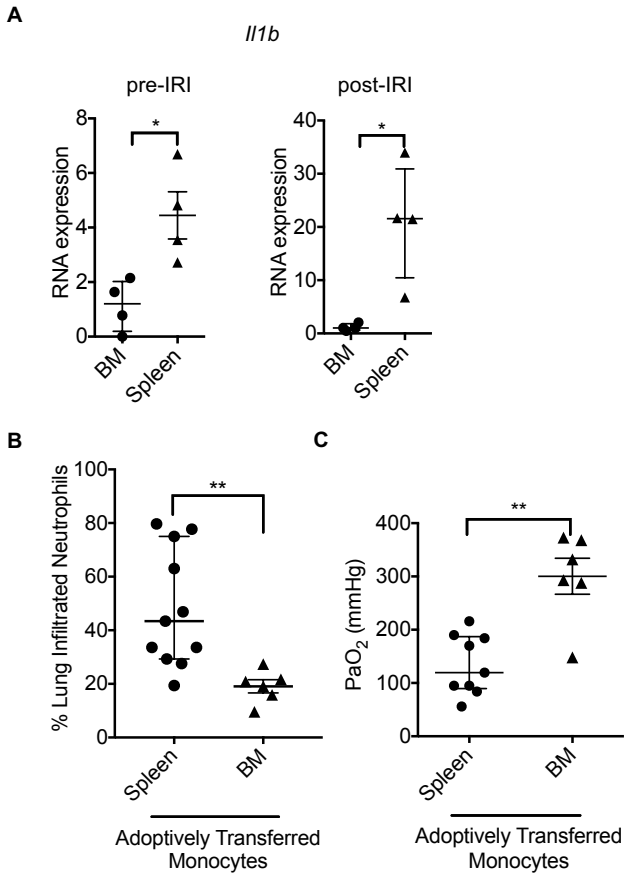

Figure S11. Effect of bone marrow and splenic classical monocytes on lung ischemia reperfusion injury (A) Recipient classical monocytes were isolated from the bone marrow or spleen in resting B6 CD45.2$^+$ mice or 2 hours after transplantation of B6 CD45.1$^+$ lungs into B6 CD45.2$^+$ recipients. Expression levels of IL-1β were analyzed by quantitative real-time PCR. Data are expressed as median with interquartile range. *n*=4 per group. *p<0.01 by Mann-Whitney U test. **(B)** Percentage of extravasated neutrophils was assessed and **(C)** arterial blood oxygenation was determined in lung grafts 24 hours after transplantation of B6 CD45.1$^+$ lungs into splenectomized B6 CD45.2$^+$ recipients that received monocytes either from spleen or bone marrow of B6 CD45.2$^+$ wildtype mice. Data are expressed as median with interquartile range. *n*=6-11 per group. **p<0.01 by Mann-Whitney U test.

Video S1. Time-lapse intravital two-photon imaging of neutrophil behavior in wildtype lung grafts two hours after transplantation into syngeneic B6 LysM-GFP hosts. Recipient LysM-GFP^{+} neutrophils (green) are recruited to the graft, adhere to the vessel wall and enter the pulmonary tissue. Pulmonary vessels appear red after intravenous injection of non-targeted 655-nm quantum dots. Scale bar: 50 μm. Relative time is displayed in hrs:min:sec. Related to Figure 5.

Video S2. Time-lapse intravital two-photon imaging of neutrophil behavior in IL-1 receptor-deficient (IL-1R KO) lung grafts two hours after transplantation into syngeneic B6 LysM-GFP hosts. Recipient LysM-GFP^{+} neutrophils (green) are recruited to the graft, where they adhere to the vessel wall and form intravascular clusters without being able to efficiently extravasate. Pulmonary vessels appear red after intravenous injection of non-targeted 655-nm quantum dots. Scale bar: 50 μm. Relative time is displayed in hrs:min:sec. Related to Figure 5.